ELSEVIER

Chemical Engineering Journal 66 (1997) 193–200

Chemical Engineering Journal

Experimental studies of catalytic partial oxidation of methane to synthesis gas in a bubbling-bed reactor

L. Mleczko, T. Wurzel

Lehrstuhl für Technische Chemie, Ruhr-Universität Bochum, D-44780 Bochum, Germany

Received 15 June 1996; accepted 25 September 1996

Abstract

The catalytic partial oxidation of methane to synthesis gas was investigated in a bubbling, laboratory-scale (inner diameter, 5 cm) fluidized-bed reactor, applying a catalyst of 1wt.%Ni–α-Al_2O_3 and undiluted feed. Over the entire range of reaction conditions (p_{CH4}/p_{O2} = 1.7–4.4; T = 680–800 °C; H_{mf} = 2, 8, 17 cm; $\tau_{mod,STP}$ = 1.2–9.6 g s ml^{-1}), stable and isothermal reactor operation, as well as yields of carbon monoxide and hydrogen near the thermodynamic equilibrium were achieved. Mass transfer limitation and solid circulation in the fluidized bed are assumed to result in a mainly reduced catalyst which promotes reforming reactions. © 1997 Elsevier Science S.A.

Keywords: Fluidization; Partial oxidation of methane; Synthesis gas

1. Introduction

The large deposits of natural gas and the growing importance of environmental protection have emphasized research in the field of converting natural gas to chemical feed stocks and liquid fuels. Because processes for the direct conversion of methane, such as oxidative coupling of methane to C_{2+} hydrocarbons or partial oxidation of methane to methanol, have not proved successful, the indirect routes are expected to be the main path for the utilization of natural gas in the future.

In the indirect routes, methane is first converted to synthesis gas (syngas). At present, syngas is produced mainly by steam reforming of methane. However, syngas production is a highly competitive field and many different alternative processes have been proposed (for a review, see [1]). The research aims pursued by the development of new processes for syngas production are low consumption of natural gas, low investment costs, the possibility of high-pressure operation, low CO_2 and NO_x emissions, and easy maintenance. One of the promising routes to achieve these targets is the catalytic partial oxidation (CPO) of methane see Eq. (1).

$$CH_4 + 0.5O_2 = CO + 2H_2 \quad \Delta_r H_{1000K} = -21.8\ \text{kJmol}^{-1} \quad (1)$$

Because this reaction exhibits mild exothermicity, i.e. high thermal and carbon efficiencies might be achieved. Furthermore, energy costs and capital investment could be reduced compared with a conventional steam-reformer by an autothermal, single-step operation. Finally, the application of a suitable catalyst should result in high yields of syngas and in the reduction of the reaction temperature.

In several studies of CPO performed in fixed-bed reactors at temperatures between 700 and 1000 °C, yields of CO and H_2 near the thermodynamic equilibrium were reported (see, for example, [2]). However, despite the mild exothermicity of reaction (1), steep temperature gradients were observed [3,4]. Moreover, catalyst deactivation occurred, as a result of carbon deposition. To explain these effects, a two-stage reaction mechanism was postulated [3,4]: in the first (exothermic) stage, oxidation of methane mainly to carbon dioxide and water takes place; in the subsequent (endothermic) stage, methane is reformed with carbon dioxide and steam. In the second stage, also deposition of carbon caused by pyrolysis of methane occurs.

As a result of the inherent properties of a fluidized bed, this reactor type seems to be very suitable for performing CPO under isothermal conditions and for preventing catalyst deactivation. However, the contact time and the rate of mass transfer between bubbles and the emulsion phase have to meet requirements demanded by the two-stage reaction mechanism described above. Also, sufficiently intensive mixing of catalyst particles has to be ensured for thermal coupling of the zones where the exothermic oxidation and the endothermic reforming reactions take place. Moreover, the deactivated catalyst particles have to be transported into the oxygen-rich distributor zone, where the carbon deposits should be combusted.

PII S1385-8947(96)03190-7

Table 1
Experimental studies of CPO in fluidized-bed reactors

Ref.	Catalyst composition and loading	Reactor		Experimental conditions				Results for X_{CH4}, S_{CO}, S_{H2} (%)
		Inner diam. (cm)	H_{mf} (cm)	T (°C)	p_{CH4}:p_{O2}:p_{N2}:p_{H2O}	d_p (μm)	u/u_{mf}	
[5]	Me–α-Al_2O_3, Me = Ni, Rh, Pt, 0.5–1 wt.%	3.2	2	650–950	2:1:4:0, 1:1:4.2:0	80	– [a]	>90, >95, >95[b]
[6]	Ni–α-Al_2O_3, 15 wt.%, 1.5 wt.%	2.4	4	700–800	2:1:2:0, 2:1:2:2	45–90	2	>90, >65, n.r.[c]
[7]	Ni–α-Al_2O_3, 0.15 wt.%, 0.0015 wt.%	2.4	4	600–800	2:1:2:1	45–90	2	>90, >65, n.r.[d]
[8]	NiO–$NiAl_2O_4$, 10% Ni nominal	3	8	750–900	2:1:1:0	110–250	2[e]	>90, >97, >97[f]
[17]	Ni(15%)–MgO,Co(12%)–MgO	3	8	400–900	1.5:1:1, 2.5:1:1	140 (Ni), 130 (Co)	3 (Ni), 4.8 (Co)	Near equilibrium in the bed, drop in the freeboard[g]

[a] Freely bubbling regime.
[b] Auto-thermal operation, with activity Rh > Ni ≫ Pt, and agglomeration of Ni and Pt catalysts above 850 °C.
[c] Reverse methane reforming in freeboard.
[d] Activity increased with metal loading.
[e] Standard conditions.
[f] Reverse methane reforming in freeboard, carbon deposition.
[g] In situ activation of the catalyst; burn-off of carbon is related to the deposition of nickel particles on the reactor wall within the freeboard zone, which catalyze back-reactions and, in turn, result in lower conversions.
n.r., not reported.

Until now, only a few experimental studies have dealt with the performance of fluidized-bed reactors for CPO. The reported results are very promising (see Table 1). In all the studies, stable and isothermal operation were achieved. Good catalytic stability and yields of syngas near thermodynamic equilibrium were obtained. However, the majority of investigations reported in Table 1 were performed by applying diluted feed and low fluidization numbers.

In the work reported in this paper, catalytic partial oxidation of methane was investigated in a vigorously bubbling bed, applying an undiluted feed. The investigations were aimed at the elucidation of the effect of the reaction conditions (temperature and partial pressures of reactants) and the hydrodynamics of the fluidized bed on the syngas yield and catalytic stability. Special attention was given to the elucidation of the effect of interphase gas exchange and solids mixing on the reaction pathway and the formation of carbon.

2. Experimental details

2.1. Catalyst

The 1 wt.%Ni–α-Al_2O_3 was prepared from α-Al_2O_3 (Janssen) using an incipient wetness technique with an aqueous solution of $Ni(NO_3)_2 \cdot 6H_2O$ (Merck). After drying for 12 h at 100°C, the catalyst precursor was calcined in air at 470 °C for 10 h. Subsequently, the catalyst was reduced for 2 h in the fluidized bed in a stream of methane at 600 °C.

2.2. Apparatus

The laboratory-scale (inner diameter, 5 cm; $H = 120$ cm) fluidized-bed reactor was made from quartz. The fluidizing gas was distributed through a porous quartz plate ($d_{pore} = 40$–90 μm). The catalytic bed ($H_{mf} = 2$–17 cm) was heated electrically through the reactor wall. A disengaging section and an internal cyclone were located at the top of the reaction zone. Thermocouples within a quartz tube were located at three axial positions in the fluidized bed. For measuring the temperature profiles, one of these thermocouples was moved along the bed axis. The product components (CO, CO_2 and H_2) and the reactants (CH_4 and O_2) were analyzed on-line by gas chromatography. The amount of water that was formed during the catalytic and non-catalytic experiments was calculated from the hydrogen balance. The accuracy of the carbon and the oxygen mass balance were always better than ±2% and ±5% respectively. A detailed description of the experimental equipment is given elsewhere [9].

2.3. Experimental conditions

The reactor was operated under atmospheric pressure. Particles from 71–160 μm in diameter (group A according to Geldart classification [19]) were selected. The reactor was operated in the vigorously bubbling regime ($u/u_{mf} = 15$, $u_{mf,800\,°C} = 0.0045$ m s^{-1}). In all the experiments, undiluted feed ($CH_4 + O_2$) was applied. The temperature was limited to 800 °C to avoid agglomeration of catalyst particles and catalyst deactivation caused by volatilization of the Ni [5,10].

2.4. Thermodynamic calculations

To compare the experimental methane conversions and the selectivities to carbon monoxide and hydrogen with those predicted by thermodynamics, thermodynamic calculations for the C–H–O system were performed, applying a free energy minimization technique. Oxygen was assumed to be converted completely via deep oxidation. Because carbon deposition was not taken into account, the C–H–O system was described with the reforming reactions of methane.

3. Results

3.1. Fluidizability and temperature profiles

Over the entire range of reaction conditions investigated, the Ni–α-Al_2O_3 catalyst was readily fluidizable, which resulted in good temperature control (see Fig. 1). In the shallow-bed experiments ($H_{mf}=2$ cm), temperature gradients up to 50 K occurred. In these experiments, the maximum of the temperature was measured in the freeboard. For higher beds ($H_{mf}=8$ and 17 cm), the catalytic bed was isothermal (see Fig. 1). However, in several experiments, temperature gradients occurred in the first 5 mm above the gas distributor ($-20<(T_{distributor}-T_{bed})<20$ K). Applying the highest bed ($H_{mf}=17$ cm), a slight decrease in the temperature in the upper part of the bed was observed.

3.2. Stability

Under all the experimental conditions, the catalyst was mechanically stable. The effect of entrainment was analyzed for three different inventories of the catalyst, which were operated for 60, 120 and 60 h. After these periods, the loss of the catalyst amounted to 4, 8 and 10 g for initial catalyst masses of 41, 160 and 330 g respectively. The Ni–α-Al_2O_3 catalyst exhibited constant catalytic activity and selectivity over these periods (see Fig. 2).

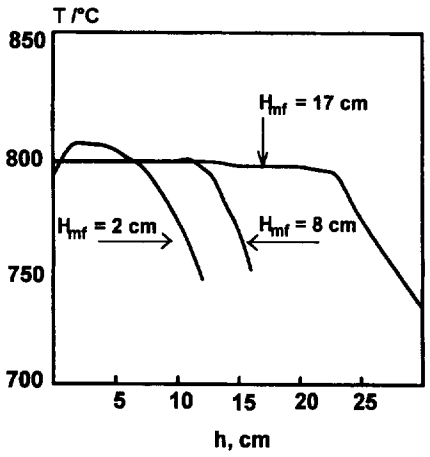

Fig. 1. Axial temperature profiles measured for different bed heights ($p_{CH4}/p_{O2}=3$; $u/u_{mf}=15$).

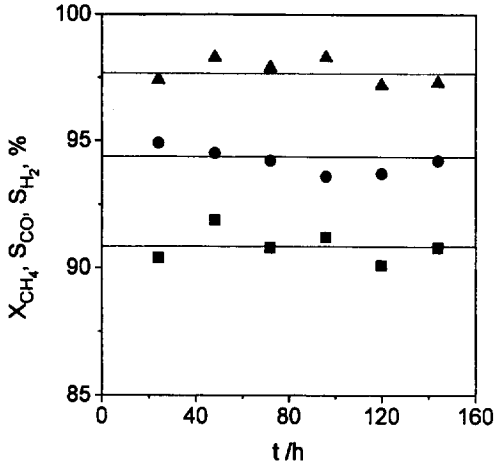

Fig. 2. Dependences of methane conversion (■), carbon monoxide (●) and hydrogen (▲) selectivity on time on stream ($T=800$°C; $p_{CH4}/p_{O2}=2$; $u/u_{mf}=15$).

3.3. Blank experiments

To check the catalytic activity of the support, methane and oxygen conversions were determined over α-Al_2O_3 particles. In this series of experiments, the reaction temperature and bed height under minimum fluidization conditions amounted to 800 °C and 8 cm respectively. The bed was fluidized with a gas velocity that corresponded to the fluidization number $u/u_{mf}=15$, applying a methane to oxygen ratio of 2:1.

In contrast to the catalytic experiments, a continuous increase in the reaction temperature along the fluidized bed was observed, resulting in a maximum temperature within the freeboard of 850 °C. This indicates that the reaction took place mainly in the freeboard. The methane and oxygen conversions amounted to 47% and 97%, respectively, whereas the yields of carbon monoxide and hydrogen were determined to 35.3% and 14.1%. After this series of experiments, the disengaging section of the reactor was covered in black deposits.

3.4. Effect of feed-gas composition and bed height

In this series of experiments, the feed-gas composition was varied between $p_{CH4}/p_{O2}=1.7$ and $p_{CH4}/p_{O2}=4.4$ for three bed heights ($H_{mf}=2$, 8, 17 cm; $m_{cat}=41$, 160, 330 g). The temperature in the bed was stabilized at 800 °C. In all the experiments, almost complete conversion of oxygen ($X_{O2}>98\%$) was achieved.

For all the bed heights and over the entire range of feed-gas compositions, the conversion of methane approached thermodynamic equilibrium (see Fig. 3(a)). The methane conversion decreased with increasing methane-to-oxygen ratio from 96.5% for $p_{CH4}/p_{O2}=1.7$ to 44.4% for $p_{CH4}/p_{O2}=4.4$. The differences between the conversions measured for the various bed heights are in the range of experimental accuracy. The selectivity to CO was higher than 90% over the entire range of reaction conditions studied in this series of experiments (see Fig. 3(b)). At low methane-to-oxygen

ratios ($p_{CH4}/p_{O2} < 2.5$), the CO selectivity approached values that corresponded to the thermodynamic equilibrium for all the bed heights. On applying higher methane-to-oxygen ratios, the CO selectivity rose as the bed height was increased. In addition, high selectivity to hydrogen ($S_{H2} > 93\%$) was measured (see Fig. 3(c)). The highest H_2 selectivity of almost 100% was measured for a methane-to-oxygen ratio of 4.4 on applying bed heights of 8 and 17 cm. For the lowest bed ($H_{mf} = 2$ cm) at high methane-to-oxygen ratios, as well as for the highest bed ($H_{mf} = 17$ cm) at low methane-to-oxygen ratios, the H_2 selectivity measured was lower than that predicted for thermodynamic equilibrium. The ratio of hydrogen to carbon monoxide in the syngas generated varied between 1.92 and 2.06; the ratio predicted by thermodynamics amounted to 2.0 for all the reaction conditions.

The data that describe the effect of the bed height on the physical properties of the catalyst, i.e. color, Brunauer–Emmett–Teller (BET) surface area (S_{BET}) and relative amount of deposited carbon (m_C/m_{cat}), are summarized in Table 2. The amount of carbon as well as the BET surface area increased with increasing bed height. Although the amount of carbon deposited is not negligible, no loss of catalytic activity or selectivity was observed (see also above).

Table 2
Effect of the bed height on the physical properties of the Ni–α-Al_2O_3 catalyst

Sample	Color	S_{BET} ($m^2\ g^{-1}$)	m_C/m_{cat} (%)
Carrier	White	< 1	0.0
Fresh cat.	Light grey	< 1	0.0
2 cm bed	Grey	< 1	0.9
8 cm bed	Dark grey	1.4	3.4
17 cm bed	Black grey	2.3	6.4

$T = 800$°C; $p_{CH4}:p_{O2} = 2:1$; $u/u_{mf} = 15$; Time on stream = 60 h.

3.5. Effect of temperature

The effect of the temperature on the catalytic performance was studied between 680 and 800 °C. The height of the bed and the methane-to-oxygen ratio in the feed gas amounted to $H_{mf} = 8$ cm ($m_{cat} = 160$ g) and $p_{CH4}/p_{O2} = 1.9$. In all the experiments, almost complete conversion of oxygen ($X_{O2} > 98\%$) was achieved.

On increasing the temperature from 700 to 800 °C, the conversion of methane rose from 75.5% to 91.3% (see Fig. 4(a)). Over the entire temperature range investigated, the conversions measured approached values predicted for

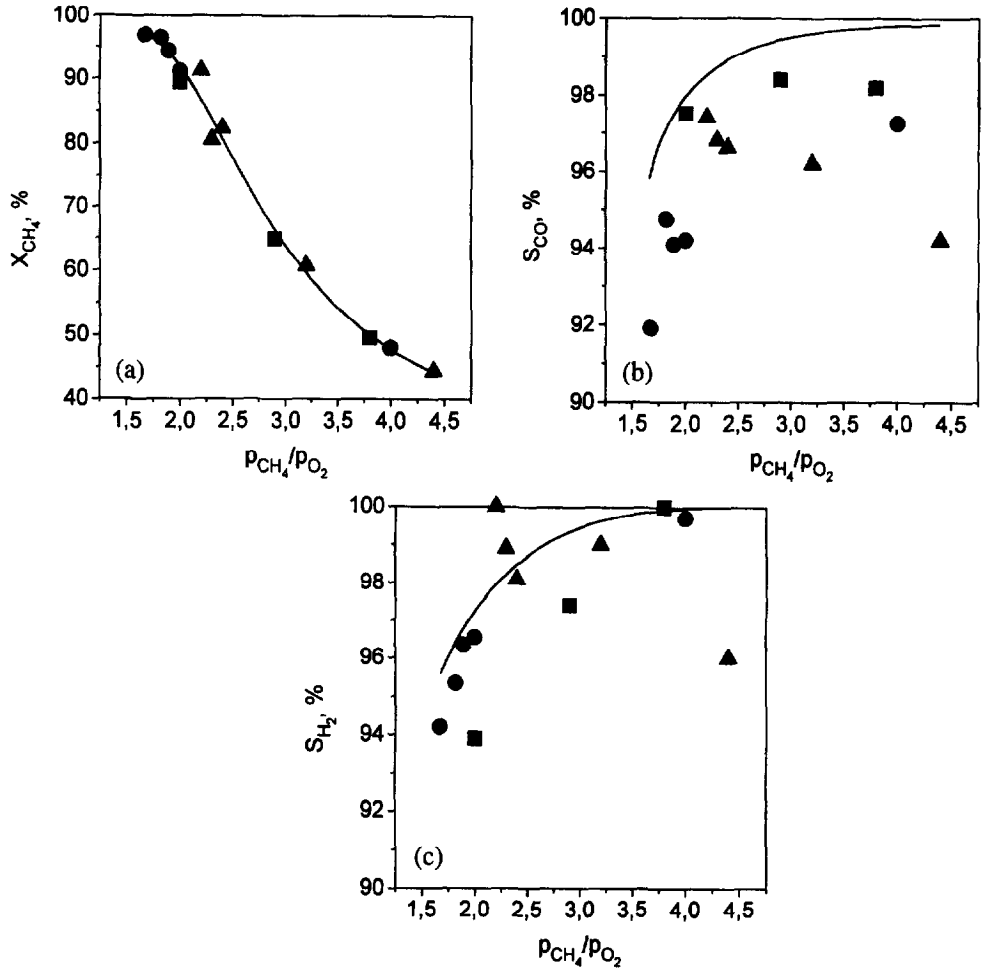

Fig. 3. Fig. 3Effect of feed-gas composition and bed height ($H_{mf} = 2$ cm (▲), $H_{mf} = 8$ cm (●), $H_{mf} = 2$ cm (■)) on (a) methane conversion, and on selectivity to (b) carbon monoxide and (c) hydrogen ($u/u_{mf} = 15$; $T = 800$ °C). Conversion and selectivity predicted by thermodynamics are shown by the full line (———).

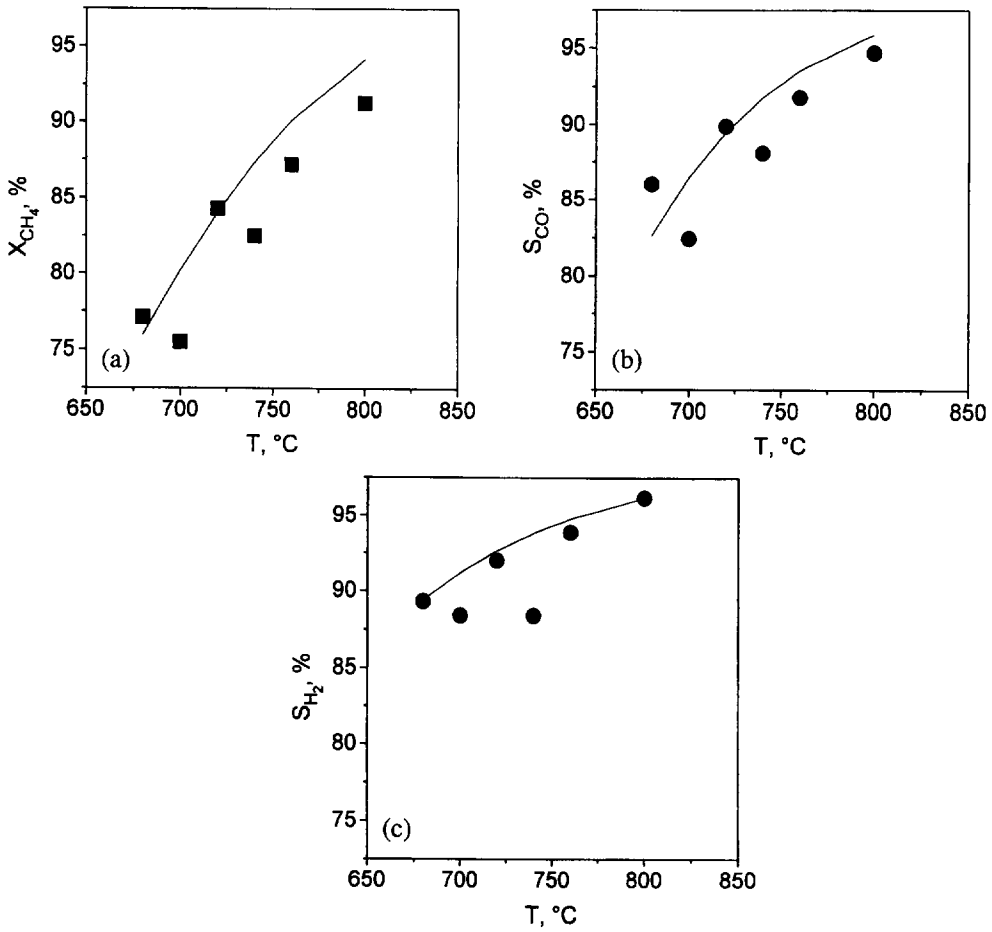

Fig. 4. Fig. 4Measured values (■) and those predicted (———) by thermodynamics for (a) methane conversion, and selectivity to (b) carbon monoxide (●) and (c) hydrogen (●), in dependence on temperature ($u/u_{mf} = 15$; $p_{CH4}/p_{O2} = 1.9$).

the thermodynamic equilibrium; the deviations between the experimental values and those predicted by thermodynamic equilibrium amounted on average to less than 2%. The selectivities to CO (see Fig. 4(b)) and to H_2 (see Fig. 4(c)) increased with temperature. At 700 °C, the CO and H_2 selectivities amounted to 82% and 88% respectively. The highest selectivities were measured at 800 °C; these amounted to $S_{CO} = 95\%$ and $S_{H2} = 96\%$. Over the entire temperature range, the average deviation from thermodynamic equilibrium was lower than 2%. The ratio of hydrogen to carbon monoxide in the syngas varied between 2.07 and 2.03; no dependence on temperature could be recognized.

3.6. Concentration profiles

To elucidate the reaction pathway of the CPO in a fluidized bed, the axial concentration profiles of each gas component were measured. In these experiments, the minimum bed height H_{mf} and the methane-to-oxygen ratio amounted to 8 cm and 2:1. The temperature of the bed and the fluidization number u/u_{mf} at the reactor inlet amounted to 800 °C and 15 respectively.

For all the concentrations, the most significant changes took place within the gas distributor zone. A steep decrease in the concentrations of the feed gases methane (Fig. 5(a)) and oxygen (Fig. 5(b)) from 66.6% and 33.3% in front of the gas distributor to 7.3% and 3.6% at a height of 1 cm in the bed was observed. Simultaneously, the highest concentration of the unselective products water (21.1%, not shown) and carbon dioxide (4.85%, Fig. 5(b)) were measured directly above the gas distributor. Furthermore, the concentrations of the selective products hydrogen and carbon monoxide (Fig. 5(a)) in the distributor zone were already remarkably high. They amounted to 51.3% and 24.5% respectively.

With increasing distance from the gas distributor, the concentration gradients decreased. Nevertheless, a continuous decrease in methane, water and carbon dioxide took place in the upper parts of the bed. In turn, further increases in hydrogen and carbon monoxide were detected. When the gas was sampled 8 cm above the gas distributor, only minor differences were detected compared with the gas composition at the reactor outlet. The H_2-to-CO ratio increased from 1 in the grid zone to approximately 2 in the upper parts of the bed.

3.7. Effect of the hydrodynamic conditions

To check the effect of the hydrodynamic conditions on the catalytic performance, the bed was fluidized by applying dif-

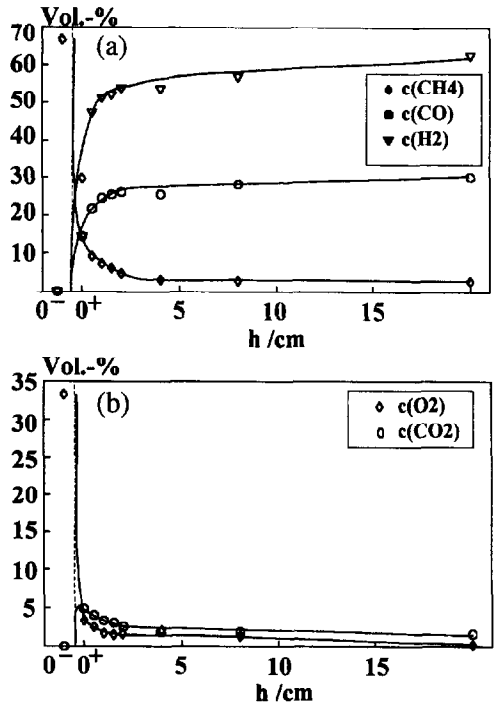

Fig. 5. Fig. 5Concentrations of (a) methane (◇), carbon monoxide (○) and hydrogen (▽) and (b) oxygen (◇) and carbon dioxide (○) in dependence on the height above the gas distributor (H_{mf}=8 cm; p_{CH4}/p_{O2}=2; T=800 °C; u/u_{mf}=15).

ferent fluidization numbers (u/u_{mf}). The bed temperature was 800 °C and the methane-to-oxygen ratio at the reactor inlet was 2. The fluidization number was varied between 10 and 23, whereas the height of the bed remained constant (H_{mf}=8 cm).

The application of different fluidization numbers led to only minor effects on the catalytic performance (see Fig. 6). The conversion and selectivity were close to those predicted by thermodynamics under all the hydrodynamic conditions applied in this series of experiments. The methane conversion varied only slightly between 90.1% and 92.4%. The same trend was measured for the selectivities to carbon monoxide and to hydrogen; they ranged from 93.6% to 94.9% and from 95.4% to 98.3% respectively. The mean deviation of the experimental data from the thermodynamic data amounted to about 1.5%.

4. Discussion

4.1. Catalytic performance

The results obtained in this study confirm that stable and isothermal operation of a fluidized-bed reactor for CPO can be obtained, even on applying undiluted feed and a high fluidization number (u/u_{mf}=15). In agreement with results reported earlier [5–8,17], the Ni–α-Al_2O_3 catalyst exhibited high activity and selectivity; almost complete oxygen and methane conversions, as well as selectivities to CO and H_2 approaching those of thermodynamic equilibrium were

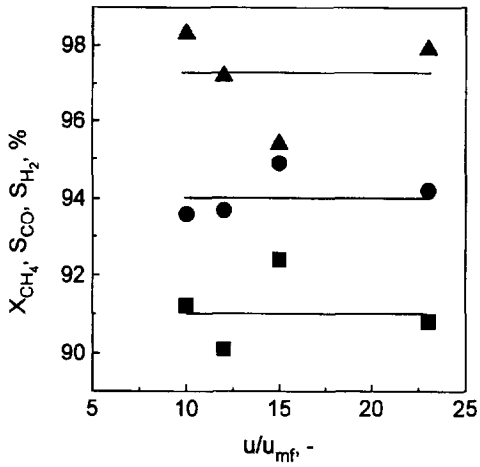

Fig. 6. Fig. 6Dependences of methane conversion (■), and selectivities to carbon monoxide (●) and to hydrogen (▲) on the fluidization number u/u_{mf} (H_{mf}=8 cm; p_{CH4}/p_{O2}=2; T=800 °C).

obtained. Because no C_{2+} hydrocarbons were detected either at the reactor outlet or when monitoring the concentration profiles, it can be concluded that gas phase reactions have only minor effects on the overall conversion. Because the methane conversion and yields of hydrogen and carbon monoxide obtained in the blank experiments were significantly lower than those during the catalytic experiments, the conclusion was drawn that the reactor performance is mainly driven by catalytic reactions. This is further confirmed by the fact that oxygen was converted rapidly in the catalytic fluidized bed, whereas the temperature increase in the freeboard observed while performing the blank experiments indicates that oxygen conversion in the fluidized bed was not complete but occurred in the freeboard.

The averaged entrainment rates up to 0.25 g h^{-1} indicate that the problem of attrition has to be elucidated in further investigations and has to be taken into account during further catalyst development. The attrition of the catalyst can promote back-reactions in the freeboard region, which subsequently result in a drop in the methane conversion [6,8,20], representing a severe source of environmental pollution.

Because syngas yields near the thermodynamic equilibrium were obtained over the entire range of reaction conditions studied in this work, optimization of the reaction temperature and feed gas composition is dictated by thermodynamics. When the reaction is carried out at 800 °C, applying a feed gas composition of CH_4:O_2=2:1, the concentration of unconverted methane in the product stream dropped to approximately 2.8%, which would be sufficiently low to utilize syngas in chemical synthesis without further gas make-up [18].

Because no decrease in the catalytic performance was observed, although carbon deposits on the catalyst were detected (see Table 2), it may be assumed that, in each case, conditions were achieved at which the rate of consumption of carbon deposits by means of combustion and Boudouard reaction was equal to the rate of carbon deposition by methane pyrolysis. However, it cannot be excluded that, as a result of

the large capacity of the catalytic bed, no effect of catalyst deactivation was observed and the true steady state of carbon deposition and carbon consumption was not achieved during these experiments. The fact that Bharadwaj and Schmidt [5] did not detect any carbon deposits during their experiments may indicate that the application of even higher rates of vertical solid mixing may completely eliminate the deposition of carbon.

4.2. Impact of the bed hydrodynamics on the reaction pathway

The steep concentration profiles indicate that reactions took place to a significant extent within the distributor zone due to the high activity of the catalyst and the excellent mass transfer conditions in this region. According to Yates [11], the height of the grid zone, which is related to the formation of bubbles, was estimated to be 1 cm ($2d_{B0}$). However, the conclusion that the rest of the catalytic bed contributes only slightly to the overall reactor performance cannot be true when considering that the concentration profiles measured by means of an immersed sampling tube represent mainly the gas concentration in the emulsion phase [25]. The visual observations confirmed that small bubbles avoid the large hydrodynamic resistance by bypassing the tube.

The high selectivity to syngas above the distributor has also been reported by other groups [6–8,17]. This effect is interpreted as the primary formation of carbon monoxide and hydrogen in the gas phase, as proposed in mechanistic and reaction engineering kinetic models of CPO over Ni, Ru or Rh catalysts (see below). The primary formation of syngas is in apparent contradiction to the studies concerning the reaction mechanism of CPO over Ni catalysts in fixed-bed reactors [3,4], in which the consecutive reaction scheme was favored. Referring to the recent mechanistic studies, it has to be mentioned that there is still no common opinion whether hydrogen and carbon monoxide are formed as primary or as secondary products. However, it is a common feature of the majority of mechanistic studies that the dissociation of methane on the active sites represents the initial step of CPO (see, for example, [12,14–16,21,23,24]). Subsequently, carbon can be directly oxidized to carbon monoxide (see, for example, [21,23]) or to carbon dioxide [15,16,21,23,24] which is converted to carbon monoxide via the Boudouard reaction with carbonaceous species [15,16,24]. Hydrogen adatoms can recombine and desorb to form hydrogen as primary product, or they can be oxidized to water by oxygen adatoms or hydroxyl groups [15,16,21,23,24].

In the light of these mechanistic studies, the high selectivity of syngas formation in a fluidized bed in the presence of oxygen can be explained by the different hydrodynamic conditions in a fixed-bed and in a fluidized-bed reactor, which affect the degree of reduction of the active sites [4,16] and the amount of oxygen adsorbed on the catalyst [21]. In a fixed-bed reactor, plug flow of gas and the high concentration of oxygen at the reactor inlet result in the oxidation of Ni to NiO, which is active for the oxidation of methane to CO_2 but not active for the reforming reactions [4]. This explanation is confirmed by the high temperature spikes caused by the exothermic deep oxidation. When the oxygen is consumed, the active sites are reduced by unconverted methane and the catalyst becomes active for the reforming reactions. In contrast, in a fluidized bed, two effects result in a very low (almost zero) concentration of oxygen within the emulsion phase where the catalytic reactions take place; only a small portion of the gas flows (u_{mf}) through the emulsion phase. The rest of the oxygen has to be supplied into the emulsion phase from bubbles by means of the interphase mass transfer. A low oxygen concentration in the emulsion phase, caused by the high reaction rates and the mass-transfer limitations between the bubble and the emulsion phase, keeps the catalyst in a reduced state. This conclusion was also confirmed by reaction engineering simulations performed for the title reaction [26].

Although the good mass-transfer conditions in the grid zone may result in a partially oxidized catalyst, the solid mixing ensures that the oxidized catalyst is transported into the upper parts of the bed, where reduction takes place, whereas the reduced catalyst is simultaneously transported down to the gas distributor. The time for the vertical mixing of solids was estimated to approximately 1.2 s [13,22]. When assuming a height of the bubble formation zone of 1 cm (see above), the catalyst remains in the oxidation zone for approximately 0.12 s, whereas the residence time in the rest of the bed amounts to about 1 s. Although the residence time is long compared with the time-scale for the chemical reactions, the circulation of particles in the bed ensures that an average reduction state of the catalyst within the emulsion phase is established and, in turn, hydrogen and carbon monoxide are formed even in the oxygen-rich distributor zone. The change in color of the catalyst samples when increasing the bed height (see Table 2) can support this explanation, because the color is assumed to stem from carbon deposits, which increase in amount with increasing degree of reduction.

Santos et al. [17] proposed an alternative model of CPO reaction in a fluidized bed, in which, as a result of the solid circulation, catalyst particles undergo periodic reduction and reoxidation. However, concentration profiles indicate that the gas composition in the emulsion phase corresponds to that in the thermodynamic equilibrium a few millimeters above the gas distributor. Consequently, the model of Santos et al. can only be applied when the reaction is not affected by mass-transfer limitation, such as bubbleless conditions or fluidization at low gas velocities.

In contrast to the results reported by the SINTEF group [6,7] and Santos et al. [8], but in agreement with the results published by Bharadwaj and Schmidt [5], no effect of the separation zone on the syngas yield at the reactor exit was detected. These findings may indicate that, under the conditions applied in this work, the contact time between the gas and the ejected solids is too short to result in a significant drop in the methane conversion, although the amount of sol-

ids in the freeboard is higher compared with the experiments performed at low fluidization numbers.

5. Conclusions

Partial oxidation (CPO) of methane was investigated in a laboratory-scale, fluidized-bed reactor, which was operated in the bubbling mode ($u/u_{mf}=15$; $\tau_{mod,STP}=4.8$ g s ml^{-1}). The results confirmed that CPO can be performed in this reactor type isothermally, applying a 1wt.%Ni–α-Al_2O_3 catalyst and undiluted feed. The catalyst was mechanically stable and readily fluidizable over the entire range of reaction conditions applied. Moreover, the catalyst exhibited constant catalytic activity, although for higher beds carbon deposition occurred. Over the entire range of reaction conditions, yields of syngas near thermodynamic equilibrium were achieved. At 800 °C and $p_{CH4}/p_{O2}=1.7$, the methane conversion amounted to 96.5%, and the selectivities to CO and H_2 amounted to 92% and 94% respectively.

The concentration profiles indicate that syngas was formed with high selectivity directly above the gas distributor. The difference between the two-stage reaction pathway in fixed-bed reactors and the reaction scheme in fluidized-bed reactors can be explained by the different hydrodynamic conditions in both reactors. It is postulated that mass-transfer limitation, as well as particle back-mixing within a fluidized bed allow the catalyst to remain in a reduced state, active for the reforming reactions.

Acknowledgements

This work was partly supported by the Commission of the European Communities (Contract JOU2-CT92-0073). The authors would like to thank Prof. Dr M. Baerns for encouraging the work and critical discussions during performing this project.

Appendix A. Notation

d_p	particle diameter (μm)
h	height (cm)
H	height of reactor/bed (cm)
m	mass (g)
p_i	partial pressure of component i (Pa)
S_{BET}	BET surface area (m^2 g^{-1})
S_i	selectivity to component i (%)
T	temperature (°C)
X_i	conversion of component i (%)

Subscripts

mf	at minimum fluidization conditions
C	carbon
cat	catalyst

References

[1] J.R. Rostrup-Nielsen, T.S. Christensen and J.-H. Bak Hansen, in A. Holmen and B.F. Magnussen (SINTEF) (Eds.), *Proc. Eurogas 94, Trondheim, 1994.*
[2] A.T. Ashcroft, A.K. Cheetham, J.S. Foord, M.L.H. Green and C.P. Grey, *Nature, 44* (1990) 319.
[3] M. Prettre, C. Eichner and M. Perrin, *Trans. Faraday Soc., 43* (1946) 33.
[4] D. Dissanayake, M.P. Rosynek, K.C.C. Kharas and J.H. Lunsford, *J. Catal., 132* (1991) 117.
[5] S.S. Bharadwaj and L.D. Schmidt, *J. Catal., 146* (1994) 11.
[6] U. Olsbye, I.M. Dahl and E. Tangstad, *Stud. Surf. Sci. Cat., 81* (1994) 303.
[7] A. Slagtern, M. Plassen and I.M. Dahl, in A. Holmen and B.F. Magnussen (SINTEF) (Eds.), *Proc. Eurogas 94, Trondheim, 1994.*
[8] A. Santos, M. Menéndez and J. Santamaria, *Catal. Today, 21* (1994) 481.
[9] L. Mleczko, R. Andorf and M. Baerns, *Chem. Ing. Tech., 62* (1990) 762.
[10] P.M. Torniainen, X. Chu and L.D. Schmidt, *J. Catal., 146* (1994) 1.
[11] J.G. Yates, *Fundamentals of Fluidized-bed Chemical Processes*, Butterworth, London, 1983, p. 113.
[12] K. Peters and E. Kappelmacher, *Brennstoff. Chem., 33* (1952) 296.
[13] M. Kwauk, *Fluidization*, Ellis Horwood, New York, 1992, p. 197.
[14] D.A. Hickman and L.D. Schmidt, *AIChE J., 39* (1993) 1164
[15] K. Walter, O.V. Buyevskaya, D. Wolf and M. Baerns, *Catal. Lett., 29* (1994) 261.
[16] O.V. Buyevskaya, D. Wolf and M. Baerns, *Catal. Lett., 29* (1994) 249.
[17] A. Santos, M. Menéndez, A. Monzón, J. Santamaria, E.E. Miró and E.A. Lombardo, *J. Catal., 158* (1996) 83.
[18] G.A. Foulds and A.J. Lapszewicz, *Catalysis 11*, Royal Society of Chemistry, London, 1994, p. 412.
[19] D. Geldart, *Powder Technol., 7* (1973) 285.
[20] P.E. Eberly, D.A. Goetsch, G.R. Say and J.M. Vargas, *European Standard EP 0 335 668 B1*, 1988.
[21] D. Wang, O. Dewaele, A.M. De Groote and G.F. Froment, *J. Catal., 159* (1996) 418.
[22] D. Geldart, *Gas Fluidization Technology*, Wiley, New York, 1986, p. 107.
[23] J.A. Lapszewicz and X.Z. Jiang, *Prep. Am. Chem. Soc. Div. Pet. Chem., 37* (1993) 3644.
[24] J.C. Slaa, R.J. Berger and G.B. Marin, *Proc. Spring ACS Meet., New Orleans, LA, 24–29 March 1996*, p. 126.
[25] D.R. van der Vaart, *Ind. Eng. Chem. Res., 31* (1992) 999.
[26] M. Baerns, O.V. Buyevskaya, L. Mleczko and D. Wolf, *Stud. Surf. Sci. Catal.*, in press.